

Enhanced Fluorescence Intermittency of CdSe-ZnS Quantum-Dot Clusters

Ming Yu and Alan Van Orden

Department of Chemistry, Colorado State University, Fort Collins, Colorado 80523, USA

(Received 23 June 2006; published 8 December 2006)

Fluorescence intermittency, or blinking, of individual close-packed clusters containing two or more CdSe-ZnS quantum dots (QDs) was investigated. The QD clusters exhibited rapid, intense blinking that was distinct from that of isolated QDs blinking independently. This enhanced blinking is suggested to occur when the QDs in the cluster become electronically coupled. The nature of this coupling is not known, though electrons trapped from QDs when they blink off may play a role by altering the electronic environment of neighboring QDs and enhancing their fluorescence properties.

DOI: [10.1103/PhysRevLett.97.237402](https://doi.org/10.1103/PhysRevLett.97.237402)

PACS numbers: 78.67.Bf, 73.21.-b, 73.50.Gr, 78.55.Et

Semiconductor quantum dots (QDs) have been studied for many years to understand their unique, size tunable optical properties and to investigate their potential applications in optoelectronic devices and biological imaging [1,2]. In particular, much effort has been devoted to the phenomenon of fluorescence intermittency, or blinking, of individual QDs [3–6]. Blinking is thought to occur when a photoexcited electron formed in the core of the QD becomes trapped in a defect site on the QD surface or external to the QD. This leaves the QD in a nonfluorescent positive charged state. The fluorescence is reestablished when the trapped electron recombines with the QD.

QDs can assemble into QD solids, thin films, chains, and clusters [7–17]. Electronic coupling between QDs in these systems, by way of Förster resonance energy transfer [7,9–11,14], exciton transfer [17], or photoinduced fluorescence enhancement (PFE) [8,12,13,16], has been observed. It is of interest to understand how such interactions affect, or are effected by, the blinking behavior of the individual QDs in the assemblies. Do the individual QDs blink independently, or can the blinking of one QD alter the blinking of neighboring QDs? The former case appears to occur in solids doped with isolated QDs [18,19], whereas the latter may arise in closed-packed QD solids and thin films [13]. However, ensemble measurements cannot address these questions directly because the blinking behavior of the individual QDs is averaged out.

We seek to address such questions by characterizing the blinking behavior of small clusters containing two or more QDs. Such systems are large enough for multiple QDs to interact but small enough so that the blinking of the individual QDs is still apparent. Toward that end, we report spatially correlated single molecule fluorescence spectroscopy and atomic force microscopy (AFM) [20] studies of individual QDs, small ensembles of isolated QDs, and small closed-packed QD clusters.

The QDs examined in this study were 2.4-nm diameter CdSe-ZnS core-shell colloidal nanoparticles capped with trioctylphosphine and trioctylphosphine oxide as stabilizing ligands. QD samples dissolved in toluene at $\sim 70 \mu\text{mol}$ were purchased from Evident Technologies (EvidotsTM,

Troy, New York). Small QD clusters were formed by treating $\sim 1 \text{ mL}$ of ~ 1 -nanomolar QDs diluted in hexane with a few microliters of methanol and allowing the solution to stand for $\sim 20 \text{ min}$. Methanol raises the polarity of the solvent, causing aggregation of the QDs by association of the hydrophobic ligands [21]. The degree of aggregation can be controlled by adjusting the QD and methanol concentrations and the incubation time. Following incubation, $\sim 60 \mu\text{L}$ of the solution was spin cast onto a mica cover slip to disperse the particles for subsequent fluorescence and AFM analysis in ambient air.

The experiment consisted of a Digital Instruments Bioscope AFM mounted on the stage of a Zeiss Axiovert inverted optical microscope. The optical microscope was operated in confocal scanning mode. A focused, 488-nm, cw laser (Novalux Protera, Model 488-15) with an average intensity at the sample of 140 W/cm^2 was used for excitation, and a piezodriven x - y scanning stage (Nanonics, Model NIS-30 SC-100/208) was used for sample positioning. The laser beam was focused onto the sample using a 1.3 numerical aperture, $40\times$ microscope objective (Zeiss Fluor). The fluorescence emission was collected by the same objective, directed through a $50\text{-}\mu\text{m}$ pinhole, filtered (488-nm notch, 650-nm short pass), and focused onto a single photon counting avalanche photodiode detector (PerkinElmer Optoelectronics, Model SPCM-AQR-14). The fluorescence from each particle was accumulated in 10-ms photon counting intervals for ten minutes using a multichannel scalar card (Becker & Hickl, Model PMS-400, Berlin).

After the fluorescence measurements were complete, the AFM, operated in tapping mode, was engaged to image the nanometer scale topography of the particles occupying the optical probe region. Spatial correlation of the AFM and fluorescence measurements was accomplished by recording excitation laser light locally scattered from the AFM probe tip (Veeco OTESPA etched silicon, force constant: $\sim 42 \text{ N/m}$, drive frequency: 250–300 kHz) [20]. The backscattered light was focused onto a photodiode detector, and the detector output was monitored using a lock-in amplifier (Stanford Research Systems, Model SR844) ref-

erenced to the drive frequency of the AFM cantilever. This resulted in an image of the optical probe region that could be coaligned with the topography image, recorded simultaneously. Coalignment of the scattered light and topography images identified the particles being probed by the optical microscope.

Figure 1 shows AFM topography images of samples containing predominantly individual isolated QDs [Fig. 1(a)] and small QD aggregates [Fig. 1(b)]. The particles were analyzed to determine their *effective* volumes. The effective volume is larger than the true particle volume due to tip convolution artifacts, which prevents us from resolving the individual QDs in the clusters. Volume histograms shown in Fig. 1 were derived from equivalent sized images of four different sample regions each. The individual QD histogram showed a single size distribution, while the QD cluster sample showed at least two subpopulations—individual QDs and QD clusters containing at least two QDs. Although there is considerable overlap between

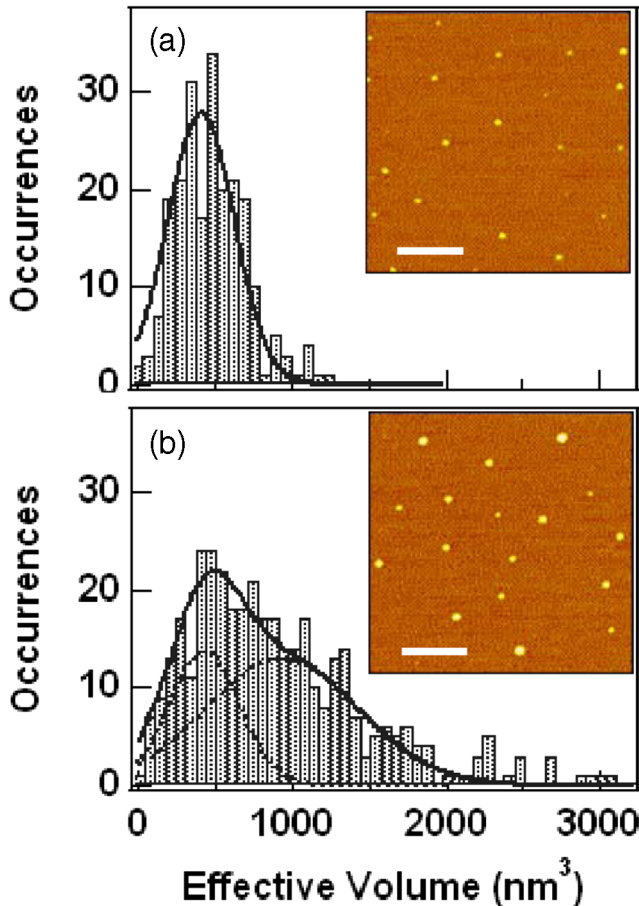


FIG. 1 (color online). AFM topography images (inset) and effective volume histograms of (a) individual isolated Evidot QDs and (b) QD clusters on mica, imaged in ambient air. The scale bars on the AFM images are 500 nm and the z height is 20 nm. The histograms were derived from four accumulated images each.

the two populations, it is found that particles with effective volumes larger than $\sim 800 \text{ nm}^3$ can be identified as QD clusters with $>90\%$ probability.

Figure 2 shows fluorescence intensity trajectories observed for several different particles or groups of particles. The corresponding AFM topography images show the regions of the sample being probed by the optical microscope while the fluorescence trajectories were recorded. In Fig. 2(a), we observed a single particle with an effective volume of 282 nm^3 in a sample that contained both single QDs and QD clusters. From the particle size, and the characteristic prolonged on and off times observed, we can identify this particle as an individual isolated QD. In samples containing predominantly individual isolated QDs, most of the fluorescent particles observed ($>80\%$) exhibited similar prolonged on- and off-time behavior.

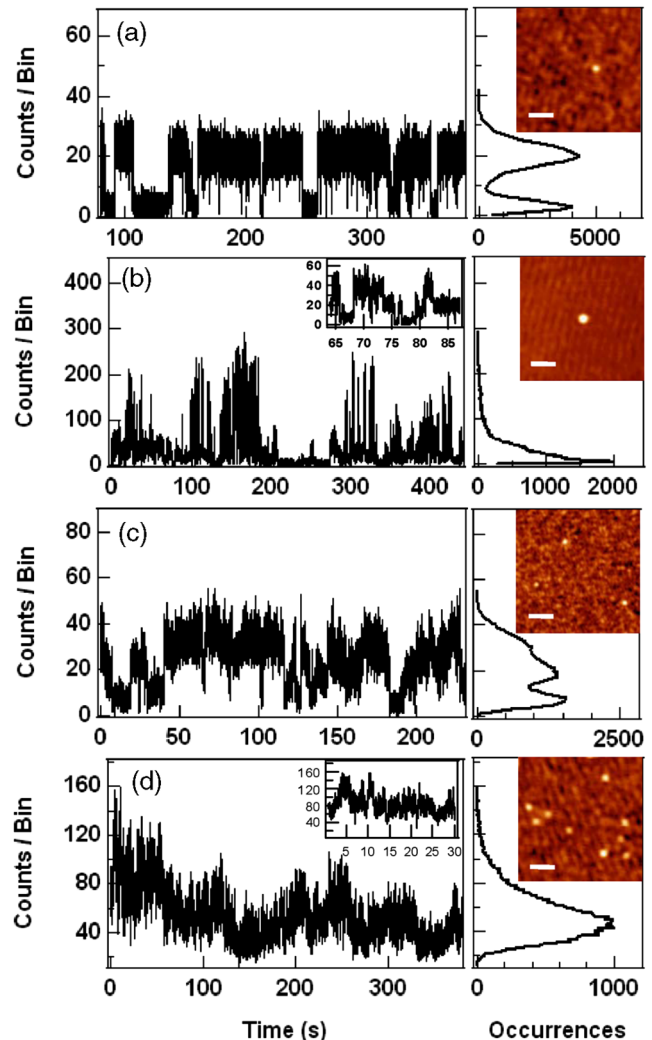


FIG. 2 (color online). Fluorescence trajectory segments (left), photon count histograms (right), and AFM topography images (inset) of (a) a single QD, (b) a QD cluster, (c) three isolated QDs, and (d) multiple isolated QDs probed simultaneously. The AFM images have scale bars of 98 nm and z ranges of 8 nm.

Figure 2(b) shows a larger particle identified in the same sample as the one shown in Fig. 2(a). This particle had an effective volume of 1380 nm^3 , identifying it as an isolated QD cluster containing two or more QDs. The fluorescence trajectory of the QD cluster differs strikingly from that of the single QD. In the lower intensity regime [Fig. 2(b), inset], the fluorescence signal shows prolonged, multistate blinking, characteristic of multiple QDs blinking independently. However, the fluorescence is dominated by extraordinary fast and intense blinking transitions, which we refer to as “enhanced” blinking.

To examine whether enhanced blinking could arise from the independent blinking of multiple QDs, we compared the fluorescence trajectories observed when two or more isolated QDs occupied the probe region of the optical microscope simultaneously. Samples that contained predominantly individual QDs were used. When three QDs were present [Fig. 2(c)] in or near the optical probe region, the fluorescence trajectory showed prolonged, multistate blinking, similar to the inset in Fig. 2(b), but no enhanced blinking was observed. When up to nine QDs were probed [Fig. 2(d)], the fluorescence trajectory showed strong fluctuations in the fluorescence intensity, but no abrupt on- or off-blinking transitions. This is the expected behavior of multiple, noninteracting QDs blinking independently.

We used autocorrelation analysis of the fluorescence trajectories to gain insight into the dynamics underlying the observed intensity fluctuations (Fig. 3). The autocorrelation function $g^{(2)}(\tau)$ is given by the equation $g^{(2)}(\tau) = \langle I(t)I(t + \tau) \rangle / \langle I(t) \rangle^2$, where $I(t)$ is the fluorescence intensity at time t , and τ is the lag time. $g^{(2)}(\tau)$ decays with increasing τ depending on the time scale at which the fluorescence signal fluctuates. For the single QD shown

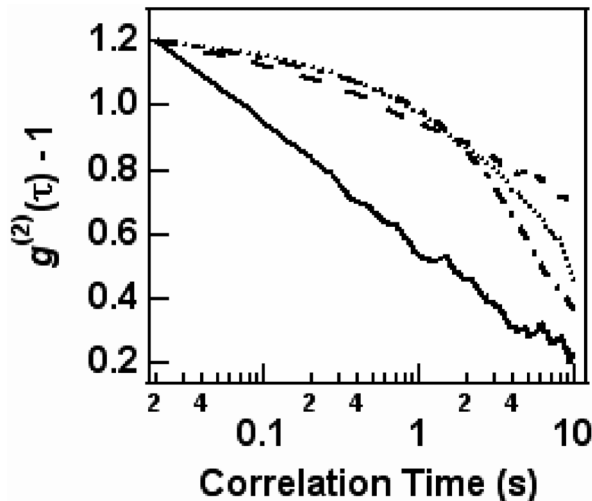


FIG. 3. Autocorrelation functions of the fluorescence trajectories shown in Fig. 2. Dashed-dotted line: single QD; solid line: QD cluster; dotted line: three isolated QDs; dashed line: multiple isolated QDs. The autocorrelation functions have been normalized to the same intensity.

in Fig. 2(a), $g^{(2)}(\tau)$ varied slowly at shorter lag times due to the prolonged on and off times (Fig. 3, dashed-dotted line). Although the absolute decay time of the autocorrelation function depends on the observation time, as well as other factors [22,23], the $g^{(2)}(\tau)$ we measured exhibits qualitative behavior characteristic of individual isolated CdSe-ZnS core-shell QDs. When multiple independent particles were probed simultaneously [Figs. 2(c) and 2(d)], the $g^{(2)}(\tau)$'s were qualitatively similar to that of the single QD (see Fig. 3). Fluorescence emission from multiple independent particles does not contribute to the decay of $g^{(2)}(\tau)$ because the emitted photons from independent particles are not correlated in time. Only the photons emitted from the same particle are correlated. Thus, the underlying dynamics captured by $g^{(2)}(\tau)$ in these situations characterizes the prolonged on and off times of the independent particles.

The autocorrelation function of the QD cluster (Fig. 3, solid line) decays precipitously from the minimum lag time. This behavior is fundamentally different from that of the isolated QDs. It shows that the rapid fluorescence intensity fluctuations observed in Fig. 2(b) are correlated in time. Hence, this behavior cannot be explained by the independent blinking of multiple QDs. We suggest that the dynamics being probed is due to the collective behavior of the QDs in the cluster.

Figure 4 summarizes our fluorescence and AFM measurements of 25 particles in a sample containing a mixture of individual QDs and QD clusters, plotted vs effective particle volume. Bars filled with horizontal lines represent particles showing exclusively two-state blinking. Bars filled with dots represent particles showing multistate blinking with prolonged on and off times but no enhanced blinking; particles showing both multistate blinking and enhanced blinking are represented by mesh filled bars.

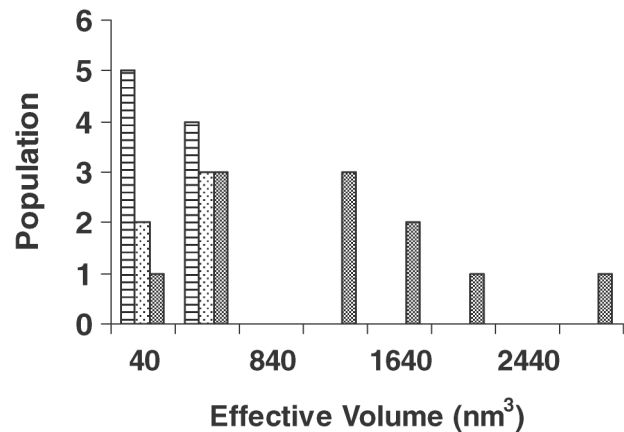


FIG. 4. A bar graph histogram summarizing the blinking behavior of 25 particles in a sample containing a mixture of individual QDs and QD clusters, plotted vs effective particle volume. Bars filled with horizontal lines represent particles showing exclusively two-state blinking. Bars filled with dots represent particles showing multistate blinking with prolonged on and off times but no enhanced blinking; particles showing both multistate blinking and enhanced blinking are represented by mesh filled bars.

ing”) and those showing both normal blinking and enhanced blinking. The classifications were based on the fluorescence trajectory and autocorrelation function observed for each particle. Importantly, all particles with volumes greater than $\sim 800 \text{ nm}^3$ exhibited enhanced blinking. These particles are identified as QD clusters based on their enlarged effective volumes. Hence, enhanced blinking is seen as a characteristic property of the QD clusters in our sample. The only particles that showed exclusively two-state blinking had effective volumes less than $\sim 600 \text{ nm}^3$, consistent with their identification as individual isolated QDs. A few of the enhanced blinking particles also had smaller effective volumes. These particles are thought to be smaller QD clusters that overlap with the single QD size distribution. Finally, some of the smaller particles showed multistate blinking but no enhanced blinking.

Our observations suggest that the QDs must be clustered together in close proximity for enhanced blinking to occur. Enhanced blinking is a transient phenomenon in which the QDs blink independently for part of the time and then rapidly switch to an enhanced blinking state at other times. We suggest that this occurs when the photoexcited QDs in the cluster become electronically coupled. At present, we can only speculate as to the nature of this coupling. One possibility is that off blinking of one QD in the cluster produces an externally trapped electron that can interact with a neighboring QD. This trapped electron may alter the electronic environment of the neighboring QD in a way that enhances its fluorescence properties. The transient nature of enhanced blinking is perhaps due to the mobility of the trapped electron, but it raises the average fluorescence intensity of the QDs over time. This could be the basis for the PFE phenomenon, which occurs in closed-packed QD films, and is believed to be caused by the buildup of trapped electrons upon continuous photoexcitation [8,12,13,16]. The trapped electrons enhance the fluorescence properties of the remaining neutral QDs in the film, but the mechanism of this enhancement is not fully understood. Our experiment may be probing an analogous PFE process that occurs at the level of the individual QDs.

In summary, individual, isolated QDs and QD clusters were analyzed using AFM and single molecule fluorescence spectroscopy. The individual QDs showed characteristic prolonged on- and off-blinking times. Multiple isolated QDs probed simultaneously showed independent blinking behavior. QD clusters exhibited enhanced blinking that is believed to arise from collective interactions of the individual QDs. One possible explanation for this observation could be that off blinking of one QD produces a

trapped electron that can enhance the fluorescence properties of the neighboring QDs.

-
- [1] V.I. Klimov, *Semiconductor and Metal Nanocrystals: Synthesis and Electronic and Optical Properties* (Marcel Dekker, New York, 2004).
 - [2] A.P. Alivisatos, W.W. Gu, and C. Larabell, *Ann. Rev. Biomed. Eng.* **7**, 55 (2005).
 - [3] M. Nirmal, B. O. Dabbousi, M. G. Bawendi, J. J. Macklin, J. K. Trautman, T. D. Harris, and L. E. Brus, *Nature (London)* **383**, 802 (1996).
 - [4] M. Kuno, D. P. Fromm, H. F. Hamann, A. Gallagher, and D. J. Nesbitt, *J. Chem. Phys.* **112**, 3117 (2000).
 - [5] M. Kuno, D. P. Fromm, S. T. Johnson, A. Gallagher, and D. J. Nesbitt, *Phys. Rev. B* **67**, 125304 (2003).
 - [6] K. Zhang, H. Y. Chang, A. H. Fu, A. P. Alivisatos, and H. Yang, *Nano Lett.* **6**, 843 (2006).
 - [7] C. R. Kagan, C. B. Murray, M. Nirmal, and M. G. Bawendi, *Phys. Rev. Lett.* **76**, 1517 (1996).
 - [8] S. Maenosono, C. D. Dushkin, S. Saito, and Y. Yamaguchi, *Jpn. J. Appl. Phys.* **39**, 4006 (2000).
 - [9] S. A. Crooker, J. A. Hollingsworth, S. Tretiak, and V. I. Klimov, *Phys. Rev. Lett.* **89**, 186802 (2002).
 - [10] Z. Y. Tang, B. Ozturk, Y. Wang, and N. A. Kotov, *J. Phys. Chem. B* **108**, 6927 (2004).
 - [11] R. Wargnier, A. V. Baranov, V. G. Maslov, V. Stsiapura, M. Artemyev, M. Pluot, and I. Nabiev, *Nano Lett.* **4**, 451 (2004).
 - [12] J. Kimura, T. Uematsu, S. Maenosono, and Y. Yamaguchi, *J. Phys. Chem. B* **108**, 13 258 (2004).
 - [13] S. Maenosono, *Chem. Phys. Lett.* **405**, 182 (2005).
 - [14] T. Franzl, A. Shavel, A. L. Rogach, N. Gaponik, T. A. Klar, A. Eychmueller, and J. Feldmann, *Small* **1**, 392 (2005).
 - [15] V. Biju, Y. Makita, A. Sonoda, H. Yokoyama, Y. Baba, and M. Ishikawa, *J. Phys. Chem. B* **109**, 13 899 (2005).
 - [16] T. Uematsu, S. Maenosono, and Y. Yamaguchi, *Appl. Phys. Lett.* **89**, 031910 (2006).
 - [17] R. Koole, P. Liljeroth, C. de Mello Donegá, D. Vanmaekelbergh, and A. Meijerink, *J. Am. Chem. Soc.* **128**, 10 436 (2006).
 - [18] I. H. Chung and M. G. Bawendi, *Phys. Rev. B* **70**, 165304 (2004).
 - [19] M. Pelton, D. G. Grier, and P. Guyot-Sionnest, *Appl. Phys. Lett.* **85**, 819 (2004).
 - [20] L. A. Kolodny, D. M. Willard, L. L. Carillo, M. W. Nelson, and A. Van Orden, *Anal. Chem.* **73**, 1959 (2001).
 - [21] C. B. Murray, D. J. Norris, and M. G. Bawendi, *J. Am. Chem. Soc.* **115**, 8706 (1993).
 - [22] R. Verberk and M. Orrit, *J. Chem. Phys.* **119**, 2214 (2003).
 - [23] G. Messin, J. P. Hermier, E. Giacobino, P. Desbiolles, and M. Dahan, *Opt. Lett.* **26**, 1891 (2001).